Raber, H. F., Heerde, T., Din, S. N. E., Flaig, C., Hilgers, F., Bitzenhofer, N., et al. (2020). Azulitox - A Pseudomonas aeruginosa P28-Derived Cancer-Cell-Specific Protein Photosensitizer. *Biomacromolecules, 21*(12), 5067-5076. doi:10.1021/acs.biomac.0c01216.

Azulitox - a Pseudomonas aeruginosa P28 derived cancer-cell specific protein-photosensitizer

Heinz Fabian Raber, Thomas Heerde, Suzanne Nour El Din, Carolin Flaig, Fabienne Hilgers, Nora Bitzenhofer, Karl-Erich Jäger, Thomas Drepper, Kay-Eberhard Gottschalk, Nicholas Emil Bodenberger, Tanja Weil, Dennis Horst Kubiczek*, and Frank Rosenau*

Azulitox – a *Pseudomonas aeruginosa* P28 derived cancer-cell specific protein-photosensitizer

Heinz Fabian Raber[‡1], Thomas Heerde[‡1], Suzanne Nour El Din[‡1], Carolin Flaig[1,4], Fabienne Hilgers[2], Nora Bitzenhofer[2], Karl-Erich Jäger[2,3], Thomas Drepper[2], Kay-Eberhard Gottschalk[4], Nicholas Emil Bodenberger[5], Tanja Weil[5], Dennis Horst Kubiczek[+1], Frank Rosenau[+1,5*]*

1. Institute for Pharmaceutical Biotechnology, Ulm University, Albert-Einstein-Allee 11, 89081 Ulm, Germany
2. Institute of Molecular Enzyme Technology, Heinrich Heine University Düsseldorf at Forschungszentrum Jülich, Stetternicher Forst, 52426 Jülich, Germany
3. Institute of Bio- and Geosciences (IBG-1: Biotechnology) Forschungszentrum Jülich, Stetternicher Forst, 52426 Jülich, Germany
4. Institute for Experimental Physics, Ulm University, Albert-Einstein-Allee 11, 89081 Ulm, Germany
5. Max Planck Institute for Polymer Research Mainz, Ackermannweg 10, 55128 Mainz, Germany

[‡,+]authors contributed equally

*corresponding authors

KEYWORDS Phototoxic protein • azurin • photosensitizer • cancer cell targeting peptide P28 • reactive oxygen species

ABSTRACT

Azulitox as a new cancer cell specific and phototoxic fusion polypeptide was generated and is composed of a photosensitizer domain and the cell-penetrating peptide P28. The photosensitizer domain (EcFbFP) was derived from a bacterial blue light receptor, which belongs to the family of light-oxygen-voltage-proteins and produces reactive oxygen species (ROS) upon excitation. P28 is derived from the cupredoxin protein azurin that is known to specifically penetrate cancer cells and bind to tumor suppressor protein p53. We show that the P28 domain specifically directs and translocates the fused photosensitizer into cancer cells. Under blue-light illumination, Azulitox significantly induced cytotoxicity. Compared to the extracellular application of EcFbFP, Azulitox caused death of about 90 % of cells as monitored by flow cytometry, which also directly correlated with the amount of ROS produced in the cells. Azulitox may pave new avenues towards targeted polypeptide-photosensitizer based photodynamic therapies with reduced systemic toxicity compared to conventional photosensitizers.

INTRODUCTION

Cancer led to 9.6 million deaths worldwide in the year 2018 and, globally, it is the cause of every 6th death.[1] Hence, cancer is one of the greatest burdens of our society. Classical available therapies and medications still have a lot of off-target effects.[1–3] Therefore, the demand for more specific cancer therapies is increasingly important and represents a growing research field.[3–12] In recent years, a variety of minimal invasive therapeutic approaches involving a combination of specific drugs and their light driven activation with selective cytotoxic activities towards cancer cells have been developed.[13] Some of these phototoxic drugs have been clinically approved for photodynamic therapy (PDT) applications.[14,15] PDT is based ideally on the local (i. e. tumor-associated)

generation of reactive oxygen species (ROS) by a phototoxic agent resulting in excessive cell damage and subsequent apoptosis upon irradiation.

In PDT, photosensitizers (PS), which are often non-toxic dye molecules, are activated by absorption of visible light. Light absorption of the PS triggers a transition from the electronic ground state to an excited singlet state and further via inter system crossing to its longer living triplet state, from which ROS production can occur via two mechanistic routes. In the type-I-reaction, the exited PS transfers an electron to molecular oxygen thereby generating a superoxide radical anion ($O_2^{\bullet-}$). A cascade of redox reactions leads to the formation of other ROS species such as hydrogen peroxide or hydroxyl radicals. The type-II-mechanism induces ROS generation by the transfer of the energy of the triplet state directly to O_2 yielding singlet oxygen.[13,16–18] In most cases, both reactions can occur simultaneously. The ratio of the reactions depends on the photophysical and photochemical properties the PS, its local environment as well as the surrounding oxygen concentration in proximity to the PS.[17] The most important promise of PDT is the opportunity to focus therapeutic activity (i. e. toxicity) to specific areas at the site of irradiation, which requires light of appropriate wavelength. The excitation wavelength directly determines the penetration depth thus defining the tissue volume, in which toxic effects are induced, as reviewed by *P. Agostinis, et al*[14] and *Dougherty T., et al*[19]. The selection of the "right" excitation light is currently still under debate. While in Europe, red light is more often used, blue light appears to be preferred in PDT in the United States.[15] The arsenal of available combinations of PS with their unique spectra properties has allowed broad applications targeting a variety of cancers. Clinical studies on various cancers indicate that both red- and blue-light absorbing PS are equally efficient and tolerable, whereas blue light seems to be more efficient for glioma cells.[15,20] Blue light has also been used in the therapy of melanoma in combination with photofrin as a photosensitizer and it

has been found to be equally efficient as red or green light with the difference that it required lower intensities[21,22]. The PDT of basal cell carcinoma BCC with blue light has been described as less painful compared to the use of red light[15]. A series of PS has already been approved by the food and drug administrations (FDA) in Europe and in Japan.[23]

Most prominent small molecule PS of the first and second generations (e. g. Photofrin®, Visudyne® or Metvix®) are derivatives of porphyrins or chlorines and they share some major therapeutic disadvantages, because they are administered systemically and possess no intrinsic specificity towards tumors or cancer cells. Patients treated with these compounds had to strictly avoid sunlight after application for 4-6 weeks to minimize potential skin damage.[24] Derivatives of 5-aminolevulinic acid are in clinical use since they show a certain inherent cancer cell specificity, but are characterized by unfavorable pharmacokinetics[25] and have been described to exhibit severe adverse effects[25,26]. In contrast, modern PS of the third generation have been equipped with additional specificity towards cancer cells or tumors by chemically conjugating tumor specific markers like antibody (-fragments)[27–29] cell surface receptor ligands[30], functionalized liposomes[31–34], immunoliposomes[35] and nanoparticles[36]. In this way, specific targeting has been achieved, which allowed reducing the effective concentrations.

Apart from the classical small molecule phototoxic drugs, a relatively new class of genetically encoded PS has emerged derived from fluorescent proteins of different origin. Most of them like KillerRed[37], KillerOrange[38] and SuperNova[39] are based on the family of green fluorescent proteins (GFP) like proteins from species DC-2005 of the *Anthomedusae* or on engineered LOV (light-oxygen-voltage) photoreceptor domains including miniSOG[40] and SOPP[41]. The class of LOV-based PS also includes EcFbFP, which was developed from the LOV domain of the *Bacillus subtilis* photoreceptor YtvA. [42] All LOV-based PS non-covalently bind flavin-mononucleotide

(FMN) as photosensitizing chromophore.[43] In a recent study, it was demonstrated that this class of genetically encoded PS is capable of efficiently producing singlet oxygen and hydrogen peroxide to a certain extent via type-I and –II reactions.[44] This process leads to an excessive oxidation of surrounding biomolecules upon excitation with blue light thus inducing phototoxicity of both bacterial or cancer target cells.[42,45–48] A promising approach in the field of PDT is the development of fully genetically encoded immunophotosensitizers that can specifically be targeted to tumor cells. Basically, these single polypeptide recombinant photosensitizers consist of synthetic fusions generated by genetic engineering and containing two domains - a targeting (e.g. antibody) and an effector (the genetically encoded PS) domain. This strategy ensures consistent PS composition and characteristics and hence exact reproducibility of its functional properties.[48] So far, different genetically encoded immunophotosensitizers have been developed using the photosensitizing proteins miniSOG and KillerRed as effector modules.[49–52] Existing targeting entities are commonly derived from single-chain variable fragment antibodies (scFvs) with a size of ~30 kDa (e.g. 4D5scFv, a stable scFv of IgG1 with specificity to HER2/neu receptors and a superior tissue penetration).[49]

A promising alternative to equip PS-polypeptides with specificity towards target cells while being smaller but offering the same oppertiunities as entities of genetically engineered fusion proteins are cell penetrating peptides (CPP). CPPs have been suggested as ideal tools for cancer therapy because they may help to overcome emerging resistances against small molecules resulting from decreased transport or increased efflux of the drug, which has been shown for CPP-conjugates methotrexate[53], taxol[54], doxorubicin[55] and bleomycin.[56] However, most CPPs penetrate cells unspecifically, which can lead to adverse side effects due to off-target distribution.[57]

In contrats, a selective CPP was derived from azurin, a member of a group of copper-containing redox proteins called cupredoxins, which not only preferentially enters cancer cells, but also leads to a stabilization of intracellular p53, resulting in higher induction of apoptosis in these cells.[58–62] A subdomain consisting of amino acids 50-77 of azurin, designated as P28 showed the same cancer cell specific penetration activity and p53 stabilization as azurin.[61,63–65] As the preclinical investigation revealed P28 is not immunogenic and showed no toxic effects in mice, thus it has the potential to be an ideal cell penetrating transport peptide.[61]

This study presents the first genetically engineered hybrid fusion of a short CPP with high cancer cells specificity and a protein photosensitizer. This novel anti-cancer polypeptide uses P28 of azurin as targeting entity and EcFbFP as a (photo-) toxic entity domain. Conventional small molecule photosensitizers provide half-lives of around 6 weeks, which requires protection of PDT patients from severe side-effects resulting from the photosensitivity.[13] In contrast, the pharmacokinetics of biologicals offer half-lives of 25 h[66] to 3-4 weeks[67] reported for small polypeptides like insulin (~6 kDa) or large IgG antibodies (~150 kDa). Thus, Azulitox (MW~19 kDa) has high potential as a new polypeptide drug for PDT as it promises a short half-life compatible with convenient reduction of undesired long term photosensitivity but also can be expected to deliver non-toxic peptide degradation products, if it is not excreted directly by renal clearance.[67] We believe that these features may be key advantages of polypeptide constructs of the Azulitox type to expand the arsenal of photosensitizers towards drugs with high efficacy and tolerability. This may pave new avenues for the development of not only efficient PDT applications, but also in combination with an increase of convenience and thus improved patients compliance.

EXPERIMENTAL SECTION

Materials

Trypsin-Ethylenediaminetetraacetic acid (EDTA) (0.05% (w/v)) sodium deoxycholate, sodium dodecyl sulfate, Tris-HCl, NaCl and 2-propanol were purchased from Sigma-Aldrich (St. Louis, Missouri, USA), fetal bovine serum, Dulbecco modified eagle medium (DMEM), Phosphate Buffered Saline (PBS), Penicillin-Streptomycin (1000U/mL), and non-essential amino acid solution (MEM) were purchased from life technologies (Carlsbad, California, USA), phalloidin-rhodamine B and propidium iodide were purchased from Thermo Fisher Scientific (Waltham, Massachusetts, USA) and Ni-NTA beads were purchased from Qiagen (Venlo, Netherlands). Statistical analysis was performed by two tailed unpaired student t-test. P values < 0.05 were considered significant. * denotes $P < 0.05$, ** < 0.01, *** $P < 0.001$ and

Methods

Cell Culture

The human lung cancer cell line A549 (ATCC®CRM-CCL-185™), respectively, were grown in DMEM supplemented with 10% FBS, 1 % minimum essential medium and 1 % penicillin streptomycin and incubated at 37 °C in a 5% CO_2 humidified incubator. Cell lines SV-52[68] and Rev2[68] were grown in DMEM with 5% FCS and incubated at 37 °C in a 5% CO_2 humidified incubator.

Plasmid constructs

The Azulitox gene was designed as a translational fusion of the P28 sequence to the carboxy-terminus of EcFbFP and chemically synthesized (Eurofins MWG, Ebersberg, Germany) and cloned into the Novagen T7 systems based on pET28a (Merck, Darmstadt, Germany. The pET28a-

EcFbFP[42] and pET28a-Azulitox were expressed in *E. coli* BL21(DE3) and purified by affinity chromatography.

Protein production and purification

A single colony was used to inoculate an overnight culture in 50 ml LB-medium containing 50 µg/ml kanamycin and 0.4 % glucose (200 rpm, 37°C). Expression cultures containing 50 µg/ml kanamycin and 0.4 % glucose were inoculated at an OD of 0.1 (30°C, 200 rpm) and induced with 0.5 mM isopropyl-β-D-thiogalactoside (IPTG) at an OD of 0.6. After induction expression cultures were grown at 200 rpm at 30 °C for 24 h. Finally, cells were harvested and centrifuged at 3000 g for 30 min at 4 °C. The resulting pellet was stored for 4 days at -80 °C. The pellet was resuspended in 15 ml lysis buffer, pH 8 containing 50 mM NaH_2PO_4, 300 mM NaCl and 15 mM imidazole followed by addition of 1 mg/ml lysozyme and incubated for 30 min on ice. Afterwards cells were mechanical disrupted by sonication for 12 min at (6 cycles, 40 %) with Bandelin SONOPULS (Berlin,Germany sonificator. The disrupted cells were centrifuged twice for 30 min at 9000 xg, 4 °C. Finally, protein was purified with a Ni-NTA column following manufacturer's instructions. After elution imidazole was removed using a Vivaspin column (10 kDa cutoff). Protein concentration and purity was determined via gel electrophoresis and BCA assay.

Fluorescence spectrum and protein activity

The fluorescence spectrum of EcFbFP and Azulitox was monitored using a Tecan fluorescence plate reader (Tecan 2000, Zurich, Switzerland). Excitation wavelength was adjusted at 450 nm and the emission was recorded between 460 and 600 nm, excitation spectra were recorded by adjusting the emission wavelength at 520 nm and scanning the excitation wavelength between 300 and

510 nm for 50 µl of 200 µM EcFbFP and Azulitox in a 96 well plate. The fluorescence of each sample was measured at an excitation wavelength of 485 nm and an emission wavelength of 530 nm in a volume of 50 µl in a 96 well plate. The quantum yields were calculated according to:

$$quantum\ yield = \frac{\int emission}{\int excitation}$$

The ROS determination of EcFbFP and Azulitox was conducted with Amplex Red from Thermo Fisher Scientific (Waltham, Massachusetts, USA), a horseradish peroxidase from Carl Roth (Karlsruhe, Germany) and a superoxide dismutase from Sigma Aldrich Aldrich (St. Louis, Missouri, USA). 50µl of each concentration of EcFbFP and Azulitox were mixed with 50µl working solution (100 µM Amplex red and 0.2 U/ml horse radish peroxidase and 4 U/ml superoxide dismutase). After an incubation of 30 min under blue light generated with a light emitting diode (488nm, Philips Lumileds, San Jose, USA). The fluorescence of each sample was measured at an excitation of 535 nm and an emission of 595 nm in a 96 well plate. The protein fluorescence of the used EcFbFP and Azulitox concentrations were measured at an excitation of 488 nm and an emission of 535 nm.

Protein uptake

2 x 10^4 human alveolar basal epithelial cells A549 (ATCC® CCL-185™) were seeded in 50 µl DMEM supplemented with 10 % FBS, 1 % minimum essential medium and 1 % penicillin streptomycin and incubated at 37 °C in a 5 % CO_2 humidified incubator in a 96 well plate and grown over night to a confluent layer. The next day, EcFbFP and Azulitox were added to reach a final concentration of 200 µM and incubated for 7 h. The supernatant was removed and stored, cells were trypsinized with 0.05% Trypsin-EDTA for 5 min at 37°C, removed from the plate and resuspended in 200 µl RIPA buffer (25 mM Tris-HCl, 150 mM NaCl, 1% sodium deoxycholate,

0.2% sodium dodecyl sulfate, pH 7.6). After 30 min, cells were centrifuged 250 xg for 5 min and the supernatant containing intracellular proteins was collected. Three samples (pure protein (200 µM), the collected supernatant and the intracellular proteins) with each 10 µl from both EcFpFP and Azulitox uptake assay were loaded on a SDS gel following Laemmli (1970).[69] After electrophoresis, the gels were silver stained following M. Chevallet et al. (2006).[70] The absence or presence of the characteristic band for EcFbFP and Azulitox respectively, allowed us to conclude whether the protein was taken up into the cells or remained in the supernatant. The integrated density of fluorescence within the cell, the cell area and the mean background fluorescence was determined with the program ImageJ (Bethesda, Maryland, USA). The mean corrected total cell fluorescence was determined (CTCF) by the following formula with sample sets of n=44 (SV-52) and n=54 (Rev2):

$$CTCF = \text{fluorescence} - (\text{cell area} * \text{mean fluorescence background}).$$

Confocal laser scanning microscopy

4 x 10^4 A549 cells were seeded in ibidi µ-slides (ibidi®, Munic, Germany) and grown overnight in 200 µl of DMEM supplemented with 10 % FBS, 1 % minimum essential medium and 1 % penicillin streptomycin and incubated at 37 °C in a 5 % CO_2 humidified incubator. Protein was added to the growth medium to reach a final concentration of 200 µl. The growth medium was removed and the cells were washed twice with pre-warmed PBS followed by incubation of the cells with 5 µl of phalloidin-rhodamine B in 195 µl PBS for 20 min in order to stain the actin cytoskeleton. Cells were washed twice with PBS and visualized with an inverted laser scanning microscope (LSM 710, Carl Zeiss Inc., Oberkochen, Germany) at a wavelength of 514 nm for rhodamine-phalloidin (red) and 488 nm for EcFbFP and Azulitox respectively (green). Via the

overlay of both images taken at 514 nm and 488 nm the internalized Azulitox fusion protein (yellow) was determined.

Kinetics of protein uptake

4 x 10^4 A549 cells were seeded in ibidi µ-slides (ibidi®, Munich, Germany) and grown overnight in 200 µl of DMEM supplemented with 10% FBS, 1% minimum essential medium and 1% penicillin streptomycin and incubated at 37 °C in a 5% CO_2 humidified incubator. The growth medium was removed and the cells were washed twice with pre-warmed PBS followed by incubation of the cells with 5 µl of phalloidin-rhodamine B in 195 µl PBS for 20 min in order to stain the actin cytoskeleton. Cells are washed twice with PBS and covered with DMEM. Cells are visualized with an inverted laser scanning microscope (LSM 710, Carl Zeiss Inc., Oberkochen, Germany) at a wavelength of 514 nm for rhodamine-phalloidin (red) and 488 nm for EcFbFP and Azulitox respectively (green). Directly after the first measurement, Azulitox is added to the medium to a final concentration of 200 µM and the increase of Azulitox in the cells is observed over a period of 7 h. Via the overlay of images taken at 514 nm and 488 nm for each time point the internalized Azulitox fusion protein (yellow) was determined.

For the following experiments, cells were permanently incubated in complete darkness in a special dark room except for the treatment with blue light.

Azulitox Uptake inhibition testing

4 x 10^4 A549 cells were seeded in ibidi µ-slides (ibidi®, Munic, Germany) and grown overnight in 200 µl of DMEM supplemented with 10 % FBS, 1 % minimum essential medium and 1 % penicillin streptomycin and incubated at 37 °C in a 5% CO_2 humidified incubator. The alveolar epithelial cancer cells (A549) were treated with monensin (0,5 mmol/L, 60 min), methyl-β-

cyclodextrin (10 mmol/L, 60min), or remained untreated, followed by incubation with Azulitox in DMEM at 37 °C under 5% CO_2 in total darkness for 7 h. The growth medium was removed and the cells were washed twice with pre-warmed PBS followed by incubation of the cells with 5 µl of phalloidin-rhodamine B in 195 µl PBS for 20 min in order to stain the actin cytoskeleton. Cells were washed twice with PBS and visualized with an inverted laser scanning microscope (LSM 710, Carl Zeiss Inc., Oberkochen, Germany) at a wavelength of 514 nm for rhodamine-phalloidin (red) and 488 nm for Azulitox respectively (green). Via the overlay of both images taken at 514 nm and 488 nm the internalized Azulitox fusion protein (yellow) was determined.

Cancer cell specific uptake of Azulitox

SV-52[68] and Rev2[68] cell lines were seeded in ibidi µ-slides (ibidi®, Munic, Germany) and grown overnight in 200 µl of DMEM supplemented with 5% FCS and incubated at 37 °C in a 5% CO_2 humidified incubator. Protein was added to the growth medium to reach a final concentration of 200 µl. The growth medium was removed and the cells were washed twice with pre-warmed PBS followed by incubation of the cells with 5 µl of phalloidin-rhodamine B in 195 µl PBS for 20 min in order to stain the actin cytoskeleton. Cells were washed twice with PBS and visualized with an inverted laser scanning microscope (LSM 710, Carl Zeiss Inc., Oberkochen, Germany) at a wavelength of 514 nm for rhodamine-phalloidin (red) and 488 nm for Azulitox respectively (green). Via the overlay of both images taken at 514 nm and 488 nm the internalized Azulitox fusion protein (yellow) was determined.

Quantification of intracellular reactive oxygen species (ROS)

To investigate the generation of intracellular reactive oxygen species, $2*10^4$ A549 cells were seeded in 50 µl DMEM supplemented with 10% FBS, 1% minimum essential medium and 1% penicillin streptomycin and incubated at 37 °C in a 5% CO_2 humidified incubator in a 96 well plate and grown over night to a confluent layer. The medium was replaced with DMEM supplemented with 25 µM, 50 µM, 100 µM, or 200 µM of either EcFbFP or Azulitox and incubated for 7h followed by addition of 10 µM of non-fluorescent, cell penetrating 2',7'-dichlorodihydrofluorescein-diacetat. 2',7'-dichlorodihydrofluorescein-diacetat is de-esterified intracellularly and turns to highly fluorescent 2′,7′-dichlorofluorescein upon oxidation via the generated ROS. To determine the effect of blue light on the generation of ROS, half of the cells were treated with a light emitting diode with 4x 83 mW (488nm, Philips Lumileds, San Jose, USA) with 6 repetitive circles of 10 sec of exposure and 30 sec of darkness, while the other half were kept in the dark. Afterwards the supernatant was removed from the cells followed by washing cells twice with PBS. The intracellular fluorescence of the oxidized 2',7'-dichlorodihydrofluorescein-diacetat was measured at an excitation wavelength of 485 nm and an emission wavelength of 535 nm at a Tecan fluorescence plate reader (Tecan 2000, Zurich, Switzerland) in 96 well plates. The higher the fluorescence the more ROS were generated.

Cytotoxicity of EcFbFP and Azulitox

2 x 10^4 A549 cells were seeded in 50 µl DMEM supplemented with 10% FBS, 1% minimum essential medium and 1% penicillin streptomycin and incubated at 37 °C in a 5% CO_2 humidified incubator in a 96 well plate and grown over night to a confluent layer. The medium was replaced with DMEM supplemented with 25 µM, 50 µM, 100 µM, or 200 µM of either EcFbFP or Azulitox

and 200 µM of P28 and incubated for 7h. To determine the effect of blue light on the cytotoxicity half of the cells were treated with a light emitting diode (488nm, Philips Lumileds, San Jose, USA) with 6 repetitive circles of 10 sec of exposure and 30 sec of darkness, the other half of the cells was left in darkness. The supernatant was removed and cells were incubated with 50 µl of 0.05% trypsin for 5 min at 37°C. Cells were removed from the plate, transferred into Eppendorf tubes and centrifuged for 3 min at 750 xg. The supernatant was removed and the cell pellet was resuspended in 200 µl binding buffer (P3566, Thermo Fisher Scientific, Waltham, Massachusetts, USA) and 4 µl propidium iodide (final concentration of 3µM) and incubated for 5 min in order to stain the dead cells. The supernatant was removed, cells were washed twice with pre-warmed PBS and transferred into a FACS tube and analyzed with a BD LSR Fortessa™ cell analyzer (BD Bioscience, Becton, 1 Becton Drive, New Jersey, USA).

RESULTS ANS DISCUSION

A synthetic gene consisting of the fused gene-sequences of EcFbFP and P28 was cloned into the commercially available T7 expression vector pET28a and then competent cells of the expression strain *E.coli* BL21(DE3) were transformed with the resulting Azulitox containing plasmid. The Azulitox polypeptide was then produced in expression cultures by expression of the synthetic gene construct for biosynthesis. After its biotechnological production, Azulitox is easily accessible to standard protein purification procedures (Scheme 1).

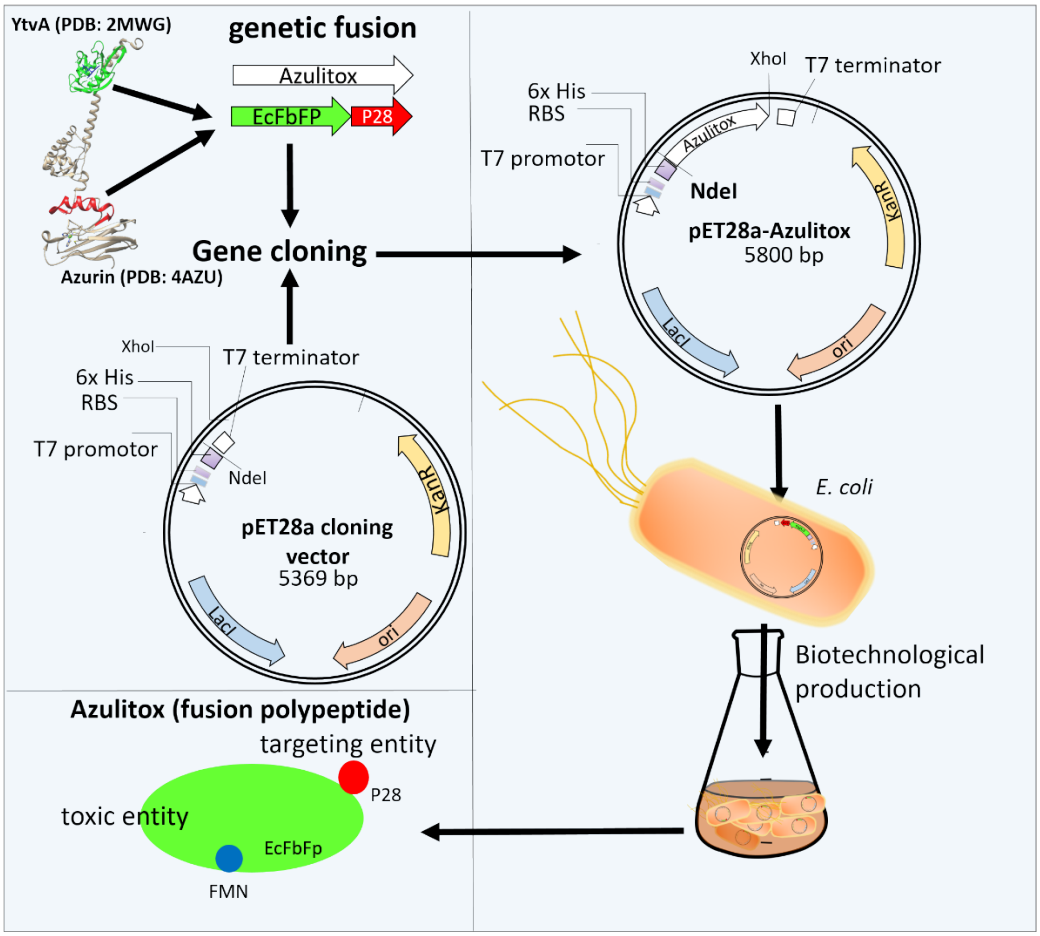

Scheme 1: Recombinant production of Azulitox. A synthetic gene encoding the sequences of EcFbFP (green) derived from YtvA (PDB: 2MWG as referenced by Jurk, M. *et al.*)[71] and P28 (red) derived from Azurin (PDB: 4AZU as referenced by Nar, H. *et al.*)[72] was cloned into a pET28a vector by enzymatic digestion with the restriction enzymes XhoI and NdeI. The vector was transformed into *E.coli* BL21(DE3) and the fusion polypeptide was overexpressed and purified by affinity chromatography.

Azulitox and EcFbFP as a control protein were expressed in *E. coli* BL21(DE3), purified by affinity chromatography and contaminations with endotoxin were measured and found to be 0.28 EU/mL for Azulitox and 0.49 EU/mL for EcFbFP at the highest concentrations used in our experiments and thus being below the current FDA limit of 0.5 EU/mL for medical devices and

parenteral drugs. Emission and excitation spectra of EcFbFP and Azulitox were measured with a fixed excitation wavelength of 450 nm for the emission spectra and a fixed emission wavelength of 520 nm for the excitation spectrum. The Azulitox fusion-protein and EcFbFP show almost identical fluorescence characteristics, similar quantum yields of 0,55 for EcFbFP and 0,5 for Azulitox and a concentration dependency of the fluorescence for both proteins (Figure 1A, B, C left) suggesting that the short P28 domain (28 aa residues) has no negative effects on EcFbFP functionality. Next, the generation of reactive oxygen species (ROS) was studied *in vitro* for Azulitox and EcFbFP by the Amplex red and peroxidase dependent assay. The generated radicals were converted into hydrogen peroxide via superoxide dismutase in this assay. In the presence of the peroxidase, Amplex red reacts with the hydrogen peroxide to the fluorescent molecule resorufin. In comparison to EcFbFP as a control Azulitox showed an almost identical dependency of the amount of ROS developed on increasing fluorescence intensities (Figure 1C right). Both curves interestingly exhibited an exponential course. This suggests a different behavior of both proteins at very high concentrations which preliminary maybe explained by a reduction of bleaching of the FMN cofactor and/or oxidative destruction of the protein background due to an increase of molecular shading in parallel to the increase of protein concentrations. To investigate if P28 facilitates the specific uptake of the PS domain into the A549 cancer cells, we first determined transport and localization of EcFbFP and Azulitox in these cells. Analysis of Azulitox uptake by Confocal laser scanning microscopy (CLSM) using the intrinsic green fluorescence of the PS domain revealed an efficient uptake of the fusion protein compared to the control EcFbFP in the A549 cancer cell line (Figure 1D). Azulitox was efficiently uptaken into these cells after 7h of incubation as depicted in the merged images of the stained cytoskeleton and the protein fluorescence. CLSM analyses of Azulitox uptake into phalloidin-rhodamine B stained A549 cells

in a 8-well µ ibidi slide over a period of 7 hours reveled a fast internalization of Azulitox already within the first hour after addition of the fusion protein as the Azulitox-specific fluorescence increased within the cells (Figure 1E). Phalloidin-rhodamin B staining uses the affinity of the death cap mushroom *Amanita phalloides* toxin phalloidin towards actin to fluorescently label the cytoscelleton and thus the cytoplasm of the cell and thus delivers optical information of their shape in CLSM. The rapid increase in fluorescence within the cells indicates a strong and efficient uptake into A549 cells. These results are consistent with the work reported by *Taylor, et al.*[60] emphasizing the importance and the vital role of the amino acids 50-77 (P28) of azurin and their significance for the cellular internalization. The cellular uptake of Azulitox was further confirmed biochemically in comparison with EcFbFP as the non-penetrating negative control protein. Cells were harvested and the cellular protein content was analyzed via SDS-PAGE and silver staining. Supernatants and the cell lysate of EcFbFP and Azulitox treated cells were used (Figure 1F). In contrast to EcFbFP, Azulitox treated cells showed that the majority of the protein was internalized and only marginal amounts remained extracellular in the supernatant. This is in accordance with previous studies, which proved that the P28 sequence is relevant for cell internalization.[62]

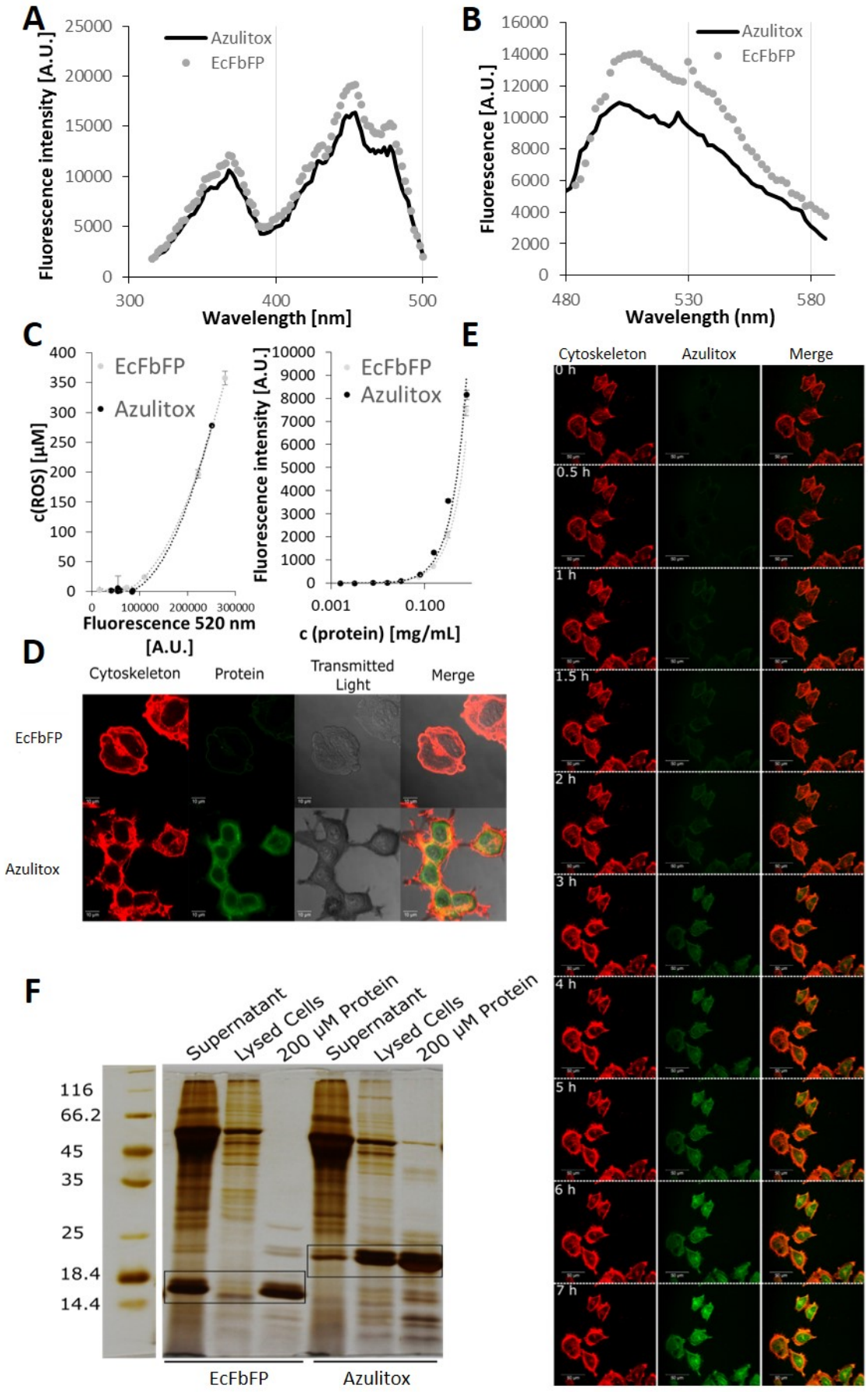

Figure 1: (A) and (B) Excitation (left) and emission (right) spectra of EcFbFP and Azulitox were measured with a fixed excitation wavelength of 450 nm for the emission spectra and a fixed emission wavelength of 520 nm for the excitation spectrum at a Tecan fluorescence reader in a 96 well plate. Quantum yields were calculated as 0,55 for EcFbFP and 0,5 for Azulitox **(C)** Fluorescence intensity at an excitation wavelength of 485 nm and an emission wavelength of 530 nm of EcFbFP and Azulitox in dependency of the protein concentration and Comparison of the ROS production of Azulitox and EcFbFP in dependency of the fluorescence intensity. **(D)** Confocal scanning microscopy of phalloidin-rhodamine B stained alveolar epithelial cancer cells (A549) after 7 h of EcFbFP and Azulitox addition (200 µM) in DMEM at 37°C, 5% CO_2 in total darkness. For excitation, a 514 nm laser was used for rhodamine B (red) and a 458 nm laser for EcFbFP and Azulitox (green) using a Zeiss Laser Scanning Microscope. **(E)** Confocal analyzes of Azulitox uptake into phalloidin-rhodamine B stained A549 cells in a 8-well µ ibidi slide over a period of 7 hours. **(F)** EcFbFP and Azulitox uptake into A549 cells after 7 hours of incubating cells in DMEM with 200 µM of EcFbFP and Azulitox, respectively. Cells were pelleted, resuspended in lysis buffer, centrifuged and proteins in the supernatant were compared with the intracellular proteins.

The selectivity of P28 for cancer cells has been shown by systematic evaluation of uptake pathways indicating caveolae uptake as the main pathway.[60,65] Very similar to the published P28 wild type peptide, Azulitox uptake depends mainly on caveolae-mediated endocytosis. The exposure to methyl-β-cyclodextrin disrupts caveolae dependend uptake via cholesterol depletion and thus reduced the Azulitox internalization as less protein fluorescence could be observed within the treated cancer cells compared to the control (Figure 2A). As reported previously, exposure of the late endosome/lysosome inhibitor monensin blocks the accumulation of the fusion protein in the cancer cell, suggesting that clathrin-dependent endocytosis may be one entry mechanism of P28 into cancer cells. (Figure 2A).[65] The successful inhibition of cell internalization with methyl-β-cyclodextrin and monensin confirms that the fusion protein Azulitox consisting of EcFbFP and P28 shares the same internalization pathways as P28 and hence the P28 transport domain appears fully intact and functional in the fusion protein. In order to prove a cancer specific internalization of the fusion peptide, Azulitox was tested on the SV-52 cancer fibroblast cell line and its revertant cell line Rev2, which is in contrast to the SV-52 a cell line with non-cancer properties.[68] Azulitox fluorescence was almost exclusively visible in the CLSM analysis in SV-52 cancer cells whereas in the Rev2 revertant as a control the fluorescence signal was only marginal (Figure 2B). This proves that Azulitox like P28 alone still has a significant preference to enter SV-52 cells similar

as P28 again indicating that P28 remained fully functional also in the presence of larger cargos like the 15.7 kDa EcFbFP photosensitizer domain in Azulitox.

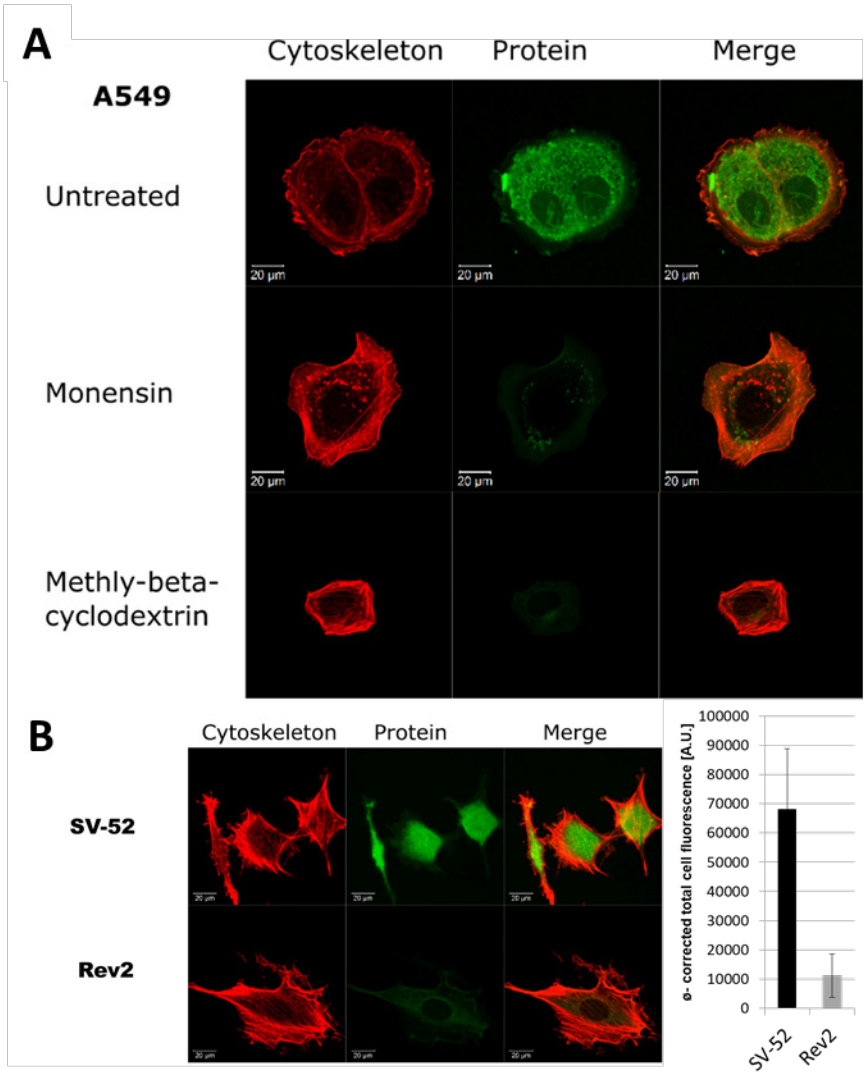

Figure 2: : **(A)** Confocal scanning microscopy of phalloidin-rhodamine B stained alveolar epithelial cancer cells (A549) treated with monensin (0.5 mmol/L, 60 min), methyl-β-cyclodextrin (10 mmol/L, 60min), or remained untreated, followed by 7 h of Azulitox uptake in DMEM at 37°C, 5% CO_2 in total darkness. **(B)** Confocal scanning microscopy of phalloidin-rhodamine B stained SV-52 and Rev2 cells after 7 h of Azulitox uptake in DMEM at 37°C, 5% CO_2 in total darkness. For excitation, a 514 nm laser was used for rhodamine B (red) and a 488 nm laser for Azulitox (green) using a Zeiss Laser Scanning Microscope. The graph shows the mean corrected total cell fluorescence of SV-52 and Rev2 cells (n= 44 SV-52 and n=54 Rev2) There is a high significant increase in uptake of Azulitox in SV-52 cancer cells ($p<0,001$) compared to the Rev2 cell line. The significance was determined by a t-test ($p> 0,05$= NS).

In the next step, phototoxicity of Azulitox was investigated by adding EcFbFP and Azulitox in increasing concentrations to the cells and incubation for 7 hours, followed by blue light irradiation of half of the samples, while the other half was kept strictly in the dark, to evaluate the effect of the additional blue-light treatment. The cytotoxicity was measured via flow cytometry, by harvesting the cells and staining them with propidium iodide (Figure 3A). Propidium iodide is a membrane impermanent and DNA intercalating reagent, which therefore only can stain permeated dead cells, caused by intracellular ROS[73] allowing fast and easy identification of live and dead cells. The EcFbFP sample ensemble showed toxicity values of below 5 % for all protein concentrations and blue-light irradiation only slightly increased the cytotoxic effect up to less than 10 % for the highest protein concentration of 200 µM. As EcFbFP alone is not internalized by the cells, ROS are likely produced at the outside. In medium, ROS could react with components of the fetal calf serum and they would not be available for the reaction with cellular membranes and even an 8-fold increase in the protein concentration did not have an impact on cellular toxicity suggesting that ROS likely reacted with medium components (Figure 3A). Azulitox on the other hand induced a significant cytotoxic effect on A549 cells. Without irradiation Azulitox caused only a low cytotoxic effect of maximum 23 %. This low dark toxicity further emphasizes the applicability of Azulitox as PS with minimal adverse effects. After irradiation with blue light, efficient cellular toxicity was observed after the application of 100 µM Azulitox and full toxicity was found in a satisfactory range for a biological at concentrations of 200 µM These experiments clearly demonstrate the superior features of Azulitox in contrast to EcFbFP providing strong phototoxic effect due to the internalization mediated by P28 and subsequent ROS formation after irradiation with blue light (Figure 3B). Additionally when Azulitox produces high concentrations

of hydrogen peroxide in the cells, the peroxide can react with superoxide anions resulting in a hydroxyl radical, which can, because of its high redox potential, oxidize molecules within a cell.[18]

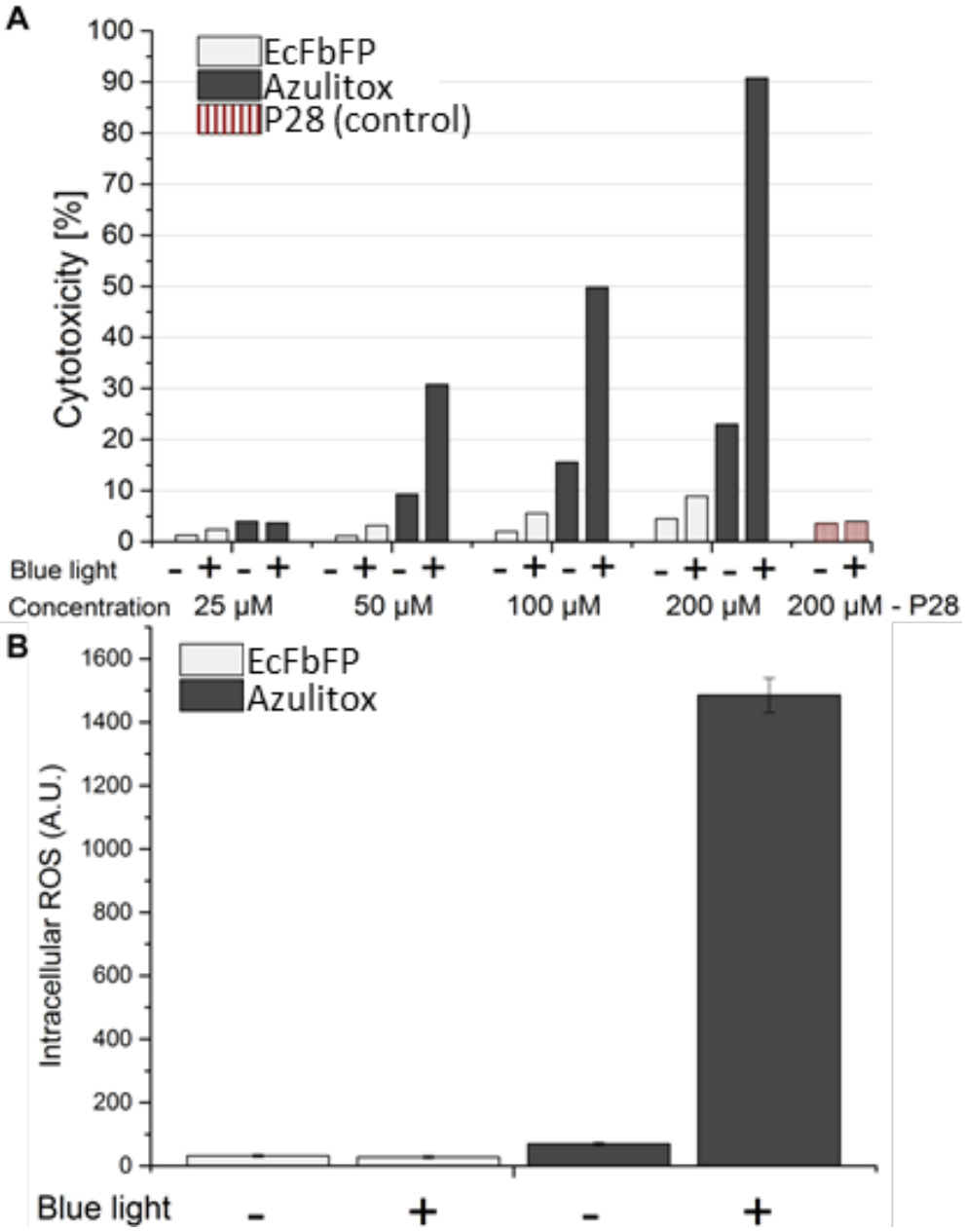

Figure 3: : **(A)** Flow cytometry analyzes of a propidium iodide stained A549 cells after incubation cells over night with 25, 50, 100 and 200 µM of EcFbFP and Azulitox respectively in total darkness. Half of the cells were treated with blue-light pulses (10 sec exposure, 30 sec pause, 6 cycles, 100mA) **(B)** Measurement of intracellular reactive oxygen species (ROS) in A549 cells after treatment of cells with 200 µM of EcFbFP and Azulitox, respectively, over night in total darkness and blue-light treatment of half of the cells (10 sec exposure, 30 sec pause, 6 cycles, 100 mA). Non-fluorescent, cell penetrating 2',7'-dichlordihydrofluorescein-diacetat is transformed into the fluorescent 2',7'-dichlorfluorescein in the cell and intracellular fluorescence is measured at an excitation wavelength of 485 nm and an emission wavelength of 535 nm. There is a high significant increase in ROS production ($p < 0{,}001$ = ***) by comparing

EcFbFP exposed to blue light and Azulitox with Azulitox exposed to blue light. The significance was determined by a t-test (p> 0,05= NS).

In summary, bifunctional photosensitizers, where the photosensitizer module is combined with a targeting domain, are promising tools for various targeted PDT approaches. The *in vivo* applicability could be further improved by using enhanced versions of the FMN-binding PS, such as DsFbFP M49I, SOPP or SOPP3, exhibiting increased ROS generation which would elevate the toxicity of next generation Azulitox. Although we currently have no dedicated immunologic data for Azulitox, which will be generated as a crucial part of our follow-up study to determine its immunogenic potential, we believe that it may inspire as a prototype continuative studies and it may open new routes towards the development of novel protein-photosensitizer drugs of targeted types of photodynamic therapies.

The flexibility of P28 mediated uptake in contrast to molecular recognition of dedicated cellular (marker) proteins may significantly contribute to the potential of PS targeting and polypeptide fusions with P28 as targeting entities represent an important amendment to the repertoire of new PS available for targeted PDT.

CONCLUSION

In summary P28 as a targeting peptide is known to preferentially enter fast growing cancer cells with high metabolic activity without the need for a specific receptor. Its ability in a fusion protein to target a toxic domain to cancer cells will thus offer general opportunities to direct cargos into a broader spectrum of different types of cancer cells.

AUTHOR INFORMATION

Author Contributions

The manuscript was written through contributions of all authors. All authors have given approval to the final version of the manuscript

ACKNOWLEDGMENT

This work was supported the Ministry of Science, Research and Arts of the state of Baden-Württemberg in the framework of the PhD program: pharmaceutical biotechnology, the Baden-Württemberg Stiftung in the framework of "Bioinspired material synthesis" and "Biofunktionelle Materialien und Oberflachen" (Nano-Mem-to-Tech), and the European Union project "Horizon 2020" (No. 686271) in the framework "AD-gut".

REFERENCES

1. WHO. Cancer https://www.who.int/news-room/fact-sheets/detail/cancer (accessed Sep 21, 2020).

2. Ferlay, J.; Soerjomataram, I.; Dikshit, R.; Eser, S.; Mathers, C.; Rebelo, M.; Parkin, D. M.; Forman, D.; Bray, F. Cancer Incidence and Mortality Worldwide: Sources, Methods and Major Patterns in GLOBOCAN 2012. *Int. J. Cancer* **2015**, *136* (5), E359–E386 DOI: 10.1002/ijc.29210.

3. Siegel, R. L.; Miller, K. D.; Jemal, A. Cancer Statistics, 2016. *CA-Cancer J. Clin.* **2016**, *66* (1), 7–30 DOI: 10.3322/caac.21332.

4. Bakhshinejad, B.; Nasiri, H. Identification of a Novel Tumor-Binding Peptide for Lung Cancer through in-Vitro Panning. *Iran. J. Pharm. Res.* **2018**, *17* (1), 396–407 DOI: 10.22037/ijpr.2018.2150.

5. Laakkonen, P.; Vuorinen, K. Homing Peptides as Targeted Delivery Vehicles. *Integr. Biol.* **2010**, *2* (7–8), 326–337 DOI: 10.1039/c0ib00013b.

6. Baudino, T. Targeted Cancer Therapy: The Next Generation of Cancer Treatment. *Curr.*

Drug Discovery Technol. **2015**, *12* (1), 3–20 DOI: 10.2174/1570163812666150602144310.

7. Iqbal, N.; Iqbal, N. Imatinib: A Breakthrough of Targeted Therapy in Cancer. *Chemother. Res. Pract.* **2014**, *2014*, 1–9 DOI: 10.1155/2014/357027.

8. Sacha, T. Imatinib in Chronic Myeloid Leukemia: An Overview. *Mediterr. J. Hematol. Infect. Dis.* **2014**, *6* (1), e2014007 DOI: 10.4084/MJHID.2014.007.

9. Panowski, S.; Bhakta, S.; Raab, H.; Polakis, P.; Junutula, J. R. Site-Specific Antibody Drug Conjugates for Cancer Therapy. *MAbs* **2014**, *6* (1), 34–45 DOI: 10.4161/mabs.27022.

10. Willett, C. G.; Boucher, Y.; Di Tomaso, E.; Duda, D. G.; Munn, L. L.; Tong, R. T.; Chung, D. C.; Sahani, D. V.; Kalva, S. P.; Kozin, S. V.; Mino, M.; Cohen, K. S.; Scadden, D. T.; Hartford, A. C.; Fischman, A. J.; Clark, J. W.; Ryan, D. P.; Zhu, A. X.; Blaszkowsky, L. S.; Chen, H. X.; Shellito, P. C.; Lauwers, G. Y.; Jain, R. K. Direct Evidence That the VEGF-Specific Antibody Bevacizumab Has Antivascular Effects in Human Rectal Cancer. *Nat. Med.* **2004**, *10* (2), 145–147 DOI: 10.1038/nm988.

11. Shuch, Brian; Linehan, B. W. M.L.; Srivasan, R. Bevacizumab. *Oncologist* **2012**, *0031* (0), 1051–1062 DOI: 10.1634/theoncologist.2011-0227.

12. Lambert, J. M.; Chari, R. V. J. Ado-Trastuzumab Emtansine (T-DM1): An Antibody-Drug Conjugate (ADC) for HER2-Positive Breast Cancer. *J. Med. Chem.* **2014**, *57* (16), 6949–6964 DOI: 10.1021/jm500766w.

13. Dolmans, D. E. J. G. J.; Fukumura, D.; Jain, R. K. Photodynamic Therapy for Cancer. *Nat. Rev. Cancer* **2003**, *3* (5), 380–387 DOI: 10.1038/nrc1071.

14. Agostinis, P.; Berg, K.; Cengel, K. A.; Foster, T. H.; Girotti, A. W.; Gollnick, S. O.; Hahn, S. M.; Hamblin, M. R.; Juzeniene, A.; Kessel, D.; Korbelik, M.; Moan, J.; Mroz, P.; Nowis, D.; Piette, J.; Wilson, B. C.; Golab, J. Photodynamic Therapy of Cancer: An Update. *CA-Cancer J. Clin.* **2011**, *61* (4), 250–281 DOI: 10.3322/caac.20114.

15. Maytin, E. V.; Kaw, U.; Ilyas, M.; Mack, J. A.; Hu, B. Blue Light versus Red Light for Photodynamic Therapy of Basal Cell Carcinoma in Patients with Gorlin Syndrome: A

Bilaterally Controlled Comparison Study. *Photodiagn. Photodyn. Ther.* **2018**, *22*, 7–13 DOI: 10.1016/j.pdpdt.2018.02.009.

16. Gomer, C. J.; Razum, N. J. Acute Skin Response in Albino Mice Following Porphyrin Photosensitization Under Oxic and Anoxic Conditions. *Photochem. Photobiol.* **1984**, *40* (4), 435–439 DOI: 10.1111/j.1751-1097.1984.tb04614.x.

17. Moan, J.; Berg, K. The Photodegradation of Porphyrins in Cells Can Be Used To Estimate the Lifetime of Singlet Oxygen. *Photochem. Photobiol.* **1991**, *53* (4), 549–553 DOI: 10.1111/j.1751-1097.1991.tb03669.x.

18. Plaetzer, K.; Krammer, B.; Berlanda, J.; Berr, F.; Kiesslich, T. Photophysics and Photochemistry of Photodynamic Therapy: Fundamental Aspects. *Lasers Med. Sci.* **2009**, *24* (2), 259–268 DOI: 10.1007/s10103-008-0539-1.

19. Dougherty, T. J.; Gomer, C. J.; Henderson, B. W.; Jori, G.; Kessel, D.; Korbelik, M.; Moan, J.; Peng, Q. Photodynamic Therapy. *J. Natl. Cancer Inst.* **1998**, *90* (12), 889–905 DOI: 10.1093/jnci/90.12.889.

20. Jamali, Z.; Hejazi, S. M.; Ebrahimi, S. M.; Moradi-Sardareh, H.; Paknejad, M. Effects of LED-Based Photodynamic Therapy Using Red and Blue Lights, with Natural Hydrophobic Photosensitizers on Human Glioma Cell Line. *Photodiagn. Photodyn. Ther.* **2018**, *21*, 50–54 DOI: 10.1016/j.pdpdt.2017.11.002.

21. Akasov, R. A.; Sholina, N. V.; Khochenkov, D. A.; Alova, A. V.; Gorelkin, P. V.; Erofeev, A. S.; Generalova, A. N.; Khaydukov, E. V. Photodynamic Therapy of Melanoma by Blue-Light Photoactivation of Flavin Mononucleotide. *Sci. Rep.* **2019**, *9* (1), 9679 DOI: 10.1038/s41598-019-46115-w.

22. Menezes, P. F. C.; Bagnato, V. S.; Johnke, R. M.; Bonnerup, C.; Sibata, C. H.; Allison, R. R.; Perussi, J. R. Photodynamic Therapy for Photogem® and Photofrin® Using Different Light Wavelengths in 375 Human Melanoma Cells. *Laser Phys. Lett.* **2007**, *4* (7), 546–551 DOI: 10.1002/lapl.200710023.

23. Baskaran, R.; Lee, J.; Yang, S. G. Clinical Development of Photodynamic Agents and

Therapeutic Applications. *Biomater. Res.* **2018**, *22* (1), 25 DOI: 10.1186/s40824-018-0140-z.

24. Sibata, C. H.; Colussi, V. C.; Oleinick, N. L.; Kinsella, T. J. Photodynamic Therapy in Oncology. *Expert Opin. Pharmacother.* **2001**, *2* (6), 917–927 DOI: 10.1517/14656566.2.6.917.

25. Donnelly, R. F.; McCarron, P. A.; Woolfson, D. A. Derivatives of 5-Aminolevulinic Acid for Photodynamic Therapy. *Perspect. Med. Chem.* **2007**, *1*, 1177391X0700100 DOI: 10.1177/1177391x0700100005.

26. Webber, J.; Kessel, D.; Fromm, D. Side Effects and Photosensitization of Human Tissues after Aminolevulinic Acid. *J. Surg. Res.* **1997**, *68* (1), 31–37 DOI: 10.1006/jsre.1997.5004.

27. Mew, D.; Wat, C. K.; Towers, G. H.; Levy, J. G. Photoimmunotherapy: Treatment of Animal Tumors with Tumor-Specific Monoclonal Antibody-Hematoporphyrin Conjugates. *J. Immunol.* **1983**, *130* (3), 1473–1477.

28. Vrouenraets, M. B.; Visser, G. W. M.; Stewart, F. A.; Stigter, M.; Oppelaar, H.; Postmus, P. E.; Snow, G. B.; Van Dongen, G. A. M. S. Development of Meta-Tetrahydroxyphenylchlorin-Monoclonal Antibody Conjugates for Photoimmunotherapy. *Cancer Res.* **1999**, *59* (7), 1505–1513.

29. Bamberg, M.; Hasan, T.; Hasan, T. Photoimmunotherapy of Human Ovarian Carcinoma Cells Ex Vivo. *Cancer Res.* **1991**, *51* (18), 4762–4767.

30. Konan, Y. N.; Gurny, R.; Allémann, E. State of the Art in the Delivery of Photosensitizers for Photodynamic Therapy. *J. Photochem. Photobiol., B* **2002**, *66* (2), 89–106 DOI: 10.1016/S1011-1344(01)00267-6.

31. Polo, L.; Valduga, G.; Jori, G.; Reddi, E. Low-Density Lipoprotein Receptors in the Uptake of Tumour Photosensitizers by Human and Rat Transformed Fibroblasts. *Int. J. Biochem. Cell Biol.* **2002**, *34* (1), 10–23 DOI: 10.1016/S1357-2725(01)00092-9.

32. Allison, B. A.; Pritchard, P. H.; Levy, J. G. Evidence for Low-Density Lipoprotein

Receptor-Mediated Uptake of Benzoporphyrin Derivative. *Br. J. Cancer* **1994**, *69* (5), 833–839 DOI: 10.1038/bjc.1994.162.

33. Richter, A. M.; Waterfield, E.; Jain, A. K.; Canaan, A. J.; Allison, B. A.; Levy, J. G. Liposomal Delivery of a Photosensitizer, Benzoporphyrin Derivative Monoacid Ring a (Bpd), To Tumor Tissue in a Mouse Tumor Model. *Photochem. Photobiol.* **1993**, *57*, 1000–1006 DOI: 10.1111/j.1751-1097.1993.tb02962.x.

34. Zhou, C.; Milanesi, C.; Jori, G. An Ultrastructural Comparative Evaluation of Tumors Photosensitized By Porphyrins Administered in Aqueous Solution, Bound To Liposomes or To Lipoproteins. *Photochem. Photobiol.* **1988**, *48* (4), 487–492 DOI: 10.1111/j.1751-1097.1988.tb02850.x.

35. Park, J. W. Liposome-Based Drug Delivery in Breast Cancer Treatment. *Breast Cancer Res.* **2002**, *4* (3), 95–99 DOI: 10.1186/bcr432.

36. Bechet, D.; Couleaud, P.; Frochot, C.; Viriot, M. L.; Guillemin, F.; Barberi-Heyob, M. Nanoparticles as Vehicles for Delivery of Photodynamic Therapy Agents. *Trends Biotechnol.* **2008**, *26* (11), 612–621 DOI: 10.1016/j.tibtech.2008.07.007.

37. Bulina, M. E.; Chudakov, D. M.; Britanova, O. V.; Yanushevich, Y. G.; Staroverov, D. B.; Chepurnykh, T. V.; Merzlyak, E. M.; Shkrob, M. A.; Lukyanov, S.; Lukyanov, K. A. A Genetically Encoded Photosensitizer. *Nat. Biotechnol.* **2006**, *24* (1), 95–99 DOI: 10.1038/nbt1175.

38. Sarkisyan, K. S.; Zlobovskaya, O. A.; Gorbachev, D. A.; Bozhanova, N. G.; Sharonov, G. V.; Staroverov, D. B.; Egorov, E. S.; Ryabova, A. V.; Solntsev, K. M.; Mishin, A. S.; Lukyanov, K. A. KillerOrange, a Genetically Encoded Photosensitizer Activated by Blue and Green Light. *PLoS One* **2015**, *10* (12), e0145287 DOI: 10.1371/journal.pone.0145287.

39. Takemoto, K.; Matsuda, T.; Sakai, N.; Fu, D.; Noda, M.; Uchiyama, S.; Kotera, I.; Arai, Y.; Horiuchi, M.; Fukui, K.; Ayabe, T.; Inagaki, F.; Suzuki, H.; Nagai, T. SuperNova, a Monomeric Photosensitizing Fluorescent Protein for Chromophore-Assisted Light Inactivation. *Sci. Rep.* **2013**, *3*, 2629 DOI: 10.1038/srep02629.

40. Shu, X.; Lev-Ram, V.; Deerinck, T. J.; Qi, Y.; Ramko, E. B.; Davidson, M. W.; Jin, Y.; Ellisman, M. H.; Tsien, R. Y. A Genetically Encoded Tag for Correlated Light and Electron Microscopy of Intact Cells, Tissues, and Organisms. *PLoS Biol.* **2011**, *9* (4), e1001041 DOI: 10.1371/journal.pbio.1001041.

41. Westberg, M.; Holmegaard, L.; Pimenta, F. M.; Etzerodt, M.; Ogilby, P. R. Rational Design of an Efficient, Genetically Encodable, Protein-Encased Singlet Oxygen Photosensitizer. *J. Am. Chem. Soc.* **2015**, *137* (4), 1632–1642 DOI: 10.1021/ja511940j.

42. Drepper, T.; Eggert, T.; Circolone, F.; Heck, A.; Krauß, U.; Guterl, J. K.; Wendorff, M.; Losi, A.; Gärtner, W.; Jaeger, K. E. Reporter Proteins for in Vivo Fluorescence without Oxygen. *Nat. Biotechnol.* **2007**, *25* (4), 443–445 DOI: 10.1038/nbt1293.

43. Möglich, A.; Moffat, K. Structural Basis for Light-Dependent Signaling in the Dimeric LOV Domain of the Photosensor YtvA. *J. Mol. Biol.* **2007**, *373* (1), 112–126 DOI: 10.1016/j.jmb.2007.07.039.

44. Endres, S.; Wingen, M.; Torra, J.; Ruiz-González, R.; Polen, T.; Bosio, G.; Bitzenhofer, N. L.; Hilgers, F.; Gensch, T.; Nonell, S.; Jaeger, K. E.; Drepper, T. An Optogenetic Toolbox of LOV-Based Photosensitizers for Light-Driven Killing of Bacteria. *Sci. Rep.* **2018**, *8* (1), 15021 DOI: 10.1038/s41598-018-33291-4.

45. Liang, J. Y.; Cheng, C. W.; Yu, C. H.; Chen, L. Y. Investigations of Blue Light-Induced Reactive Oxygen Species from Flavin Mononucleotide on Inactivation of E. Coli. *J. Photochem. Photobiol., B* **2015**, *143*, 82–88 DOI: 10.1016/j.jphotobiol.2015.01.005.

46. Jaeger, K. E.; Drepper, T.; Endres, S.; Potzkei, J. Lov-Domain Protein for Photosensitive Defunctionalization. US20130230885A1, 2010.

47. Hilgers, F.; Bitzenhofer, N. L.; Ackermann, Y.; Burmeister, A.; Grünberger, A.; Jaeger, K. E.; Drepper, T. Genetically Encoded Photosensitizers as Light-Triggered Antimicrobial Agents. *Int. J. Mol. Sci.* **2019**, *20* (18), 4608 DOI: 10.3390/ijms20184608.

48. Souslova, E. A.; Mironova, K. E.; Deyev, S. M. Applications of Genetically Encoded Photosensitizer MiniSOG: From Correlative Light Electron Microscopy to

Immunophotosensitizing. *J. Biophotonics* **2017**, *10* (3), 338–352 DOI: 10.1002/jbio.201600120.

49. Serebrovskaya, E. O.; Edelweiss, E. F.; Stremovskiy, O. A.; Lukyanov, K. A.; Chudakov, D. M.; Deyev, S. M. Targeting Cancer Cells by Using an Antireceptor Antibody-Photosensitizer Fusion Protein. *Proc. Natl. Acad. Sci. U. S. A.* **2009**, *106* (23), 9221–9225 DOI: 10.1073/pnas.0904140106.

50. Mironova, K. E.; Proshkina, G. M.; Ryabova, A. V.; Stremovskiy, O. A.; Lukyanov, S. A.; Petrov, R. V.; Deyev, S. M. Genetically Encoded Immunophotosensitizer 4D5scFv-MiniSOG Is a Highly Selective Agent for Targeted Photokilling of Tumor Cells in Vitro. *Theranostics* **2013**, *3* (11), 831–840 DOI: 10.7150/thno.6715.

51. Proshkina, G. M.; Shilova, O. N.; Ryabova, A. V.; Stremovskiy, O. A.; Deyev, S. M. A New Anticancer Toxin Based on HER2/Neu-Specific DARPin and Photoactive Flavoprotein MiniSOG. *Biochimie* **2015**, *118*, 116–122 DOI: 10.1016/j.biochi.2015.08.013.

52. Mironova, K. E.; Chernykh, O. N.; Ryabova, A. V.; Stremovskiy, O. A.; Proshkina, G. M.; Deyev, S. M. Highly Specific Hybrid Protein DARPin-MCherry for Fluorescent Visualization of Cells Overexpressing Tumor Marker HER2/Neu. *Biochemistry (Moscow)* **2014**, *79* (12), 1391–1396 DOI: 10.1134/S0006297914120141.

53. Lindgren, M.; Rosenthal-Aizman, K.; Saar, K.; Eiríksdóttir, E.; Jiang, Y.; Sassian, M.; Östlund, P.; Hällbrink, M.; Langel, Ü. Overcoming Methotrexate Resistance in Breast Cancer Tumour Cells by the Use of a New Cell-Penetrating Peptide. *Biochem. Pharmacol.* **2006**, *71* (4), 416–425 DOI: 10.1016/j.bcp.2005.10.048.

54. Dubikovskaya, E. A.; Thorne, S. H.; Pillow, T. H.; Contag, C. H.; Wender, P. A. Overcoming Multidrug Resistance of Small-Molecule Therapeutics through Conjugation with Releasable Octaarginine Transporters. *Proc. Natl. Acad. Sci. U. S. A.* **2008**, *105* (34), 12128–12133 DOI: 10.1073/pnas.0805374105.

55. Aroui, S.; Mili, D.; Brahim, S.; Waard, M. De; Kenani, A. Doxorubicin Coupled to Penetratin Promotes Apoptosis in CHO Cells by a Mechanism Involving C-Jun NH2-

Terminal Kinase. *Biochem. Biophys. Res. Commun.* **2010**, *396* (4), 908–914 DOI: 10.1016/j.bbrc.2010.05.020.

56. Koshkaryev, A.; Piroyan, A.; Torchilin, V. P. Bleomycin in Octaarginine-Modified Fusogenic Liposomes Results in Improved Tumor Growth Inhibition. *Cancer Lett.* **2013**, *334* (2), 293–301 DOI: 10.1016/j.canlet.2012.06.008.

57. Kristensen, M.; Birch, D.; Nielsen, H. M. Applications and Challenges for Use of Cell-Penetrating Peptides as Delivery Vectors for Peptide and Protein Cargos. *Int. J. Mol. Sci.* **2016**, *17* (2), 185 DOI: 10.3390/ijms17020185.

58. Yamada, T.; Goto, M.; Punj, V.; Zaborina, O.; Chen, M. L.; Kimbara, K.; Majumdar, D.; Cunningham, E.; Das Gupta, T. K.; Chakrabarty, A. M. Bacterial Redox Protein Azurin, Tumor Suppressor Protein P53, and Regression of Cancer. *Proc. Natl. Acad. Sci. U. S. A.* **2002**, *99* (22), 14098–14103 DOI: 10.1073/pnas.222539699.

59. Yamada, T.; Fialho, A. M.; Punj, V.; Bratescu, L.; Das Gupta, T. K.; Chakrabarty, A. M. Internalization of Bacterial Redox Protein Azurin in Mammalian Cells: Entry Domain and Specificity. *Cell. Microbiol.* **2005**, *7* (10), 1418–1431 DOI: 10.1111/j.1462-5822.2005.00567.x.

60. Taylor, B. N.; Mehta, R. R.; Yamada, T.; Lekmine, F.; Christov, K.; Chakrabarty, A. M.; Green, A.; Bratescu, L.; Shilkaitis, A.; Beattie, C. W.; Das Gupta, T. K. Noncationic Peptides Obtained from Azurin Preferentially Enter Cancer Cells. *Cancer Res.* **2009**, *69* (2), 537–546 DOI: 10.1158/0008-5472.CAN-08-2932.

61. Jia, L.; Gorman, G. S.; Coward, L. U.; Noker, P. E.; McCormick, D.; Horn, T. L.; Harder, J. B.; Muzzio, M.; Prabhakar, B.; Ganesh, B.; Das Gupta, T. K.; Beattie, C. W. Preclinical Pharmacokinetics, Metabolism, and Toxicity of Azurin-P28 (NSC745104) a Peptide Inhibitor of P53 Ubiquitination. *Cancer Chemother. Pharmacol.* **2011**, *68* (2), 513–524 DOI: 10.1007/s00280-010-1518-3.

62. Chakrabarty, A. M. Bacterial Proteins: A New Class of Cancer Therapeutics. *J. Commer. Biotechnol.* **2012**, *18* (1), 4–10 DOI: 10.5912/jcb.466.

63. Yamada, T.; Christov, K.; Shilkaitis, A.; Bratescu, L.; Green, A.; Santini, S.; Bizzarri, A. R.; Cannistraro, S.; Gupta, T. K. D.; Beattie, C. W. P28, A First in Class Peptide Inhibitor of Cop1 Binding to P53. *Br. J. Cancer* **2013**, *108* (12), 2495–2504 DOI: 10.1038/bjc.2013.266.

64. Warso, M. A.; Richards, J. M.; Mehta, D.; Christov, K.; Schaeffer, C.; Rae Bressler, L.; Yamada, T.; Majumdar, D.; Kennedy, S. A.; Beattie, C. W.; Das Gupta, T. K. A First-in-Class, First-in-Human, Phase i Trial of P28, a Non-HDM2-Mediated Peptide Inhibitor of P53 Ubiquitination in Patients with Advanced Solid Tumours. *Br. J. Cancer* **2013**, *108* (5), 1061–1070 DOI: 10.1038/bjc.2013.74.

65. Yamada, T.; Mehta, R. R.; Lekmine, F.; Christov, K.; King, M. L.; Majumdar, D.; Shilkaitis, A.; Green, A.; Bratescu, L.; Beattie, C. W.; Das Gupta, T. K. A Peptide Fragment of Azurin Induces a P53-Mediated Cell Cycle Arrest in Human Breast Cancer Cells. *Mol. Cancer Ther.* **2009**, *8* (10), 2947–2958 DOI: 10.1158/1535-7163.MCT-09-0444.

66. Heise, T.; Nosek, L.; Bøttcher, S. G.; Hastrup, H.; Haahr, H. Ultra-Long-Acting Insulin Degludec Has a Flat and Stable Glucose-Lowering Effect in Type 2 Diabetes. *Diabetes, Obes. Metab.* **2012**, *14* (10), 944–950 DOI: 10.1111/j.1463-1326.2012.01638.x.

67. Zhao, L.; Ren, T. H.; Wang, D. D. Clinical Pharmacology Considerations in Biologics Development. *Acta Pharmacol. Sin.* **2012**, *33* (11), 1339–1347 DOI: 10.1038/aps.2012.51.

68. Bauer, M.; Guhl, E.; Graessmann, M.; Graessmann, A. Cellular Mutation Mediates T-Antigen-Positive Revertant Cells Resistant to Simian Virus 40 Transformation but Not to Retransformation by Polyomavirus and Adenovirus Type 2. *J. Virol.* **1987**, *61* (6), 1821–1827 DOI: 10.1128/jvi.61.6.1821-1827.1987.

69. Laemmli, U. K. Cleavage of Structural Proteins during the Assembly of the Head of Bacteriophage T4. *Nature* **1970**, *227* (5259), 680–685 DOI: 10.1038/227680a0.

70. Chevallet, M.; Luche, S.; Rabilloud, T. Silver Staining of Proteins in Polyacrylamide Gels. *Nat. Protoc.* **2006**, *1* (4), 1852–1858 DOI: 10.1038/nprot.2006.288.

71. Jurk, M., Dorn, M., Reichenwallner, J., Bardiaux, B., Hinderberger, D., Schmieder, P.

RCSB PDB - 2MWG: Full-Length Solution Structure Of YtvA, a LOV-Photoreceptor Protein and Regulator of Bacterial Stress Response https://www.rcsb.org/structure/2MWG (accessed Oct 18, 2020) DOI: 10.2210/pdb2MWG/pdb.

72. Nar, H.; Messerschmidt, A.; Huber, R.; van de Kamp, M.; Canters, G. W. Crystal Structure Analysis of Oxidized Pseudomonas Aeruginosa Azurin at PH 5·5 and PH 9·0. A PH-Induced Conformational Transition Involves a Peptide Bond Flip. *J. Mol. Biol.* **1991**, *221* (3), 765–772 DOI: 10.1016/0022-2836(91)80173-R.

73. Nicoletti, I.; Migliorati, G.; Pagliacci, M. C.; Grignani, F.; Riccardi, C. A Rapid and Simple Method for Measuring Thymocyte Apoptosis by Propidium Iodide Staining and Flow Cytometry. *J. Immunol. Methods* **1991**, *139* (2), 271–279 DOI: 10.1016/0022-1759(91)90198-O.

TABLE OF CONTENT

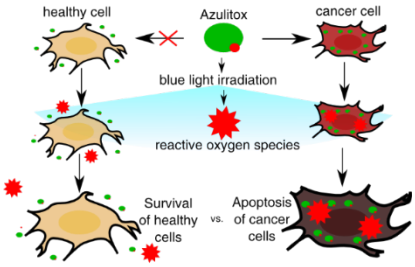

Phototoxicity and new specificity of Azulitox towards cancer-cells by translational fusion of the genetically encoded PS EcFbFP (green) and the CPP p28 (red). The CPP P28 enables the PS to preferentially enter cancer cells to then produce intracellular ROS upon irradiation with blue light, which causes cell death. Due to the cancer cell specificity of Azulitox healthy human cells are not affected by the local extracellular production of ROS and Azulitox is thus expected to possess lowered off target-effects as compared to the potential use of the PS EcFbFP alone.